

# Effect of collagen II coating on mesenchymal stem cell adhesion on chitosan and on reacylated chitosan fibrous scaffolds

Guillaume R. Ragetly · Dominique J. Griffon ·  
Hae-Beom Lee · Yong Sik Chung

Received: 15 September 2009 / Accepted: 5 May 2010 / Published online: 25 May 2010  
© Springer Science+Business Media, LLC 2010

**Abstract** The biocompatibility and biomimetic properties of chitosan make it attractive for tissue engineering but its use is limited by its cell adhesion properties. Our objectives were to produce and characterize chitosan and reacylated-chitosan fibrous scaffolds coated with type II collagen and to evaluate the effect of these chemical modifications on mesenchymal stem cell (MSC) adhesion. Chitosan and reacylated-chitosan scaffolds obtained by a wet spinning method were coated with type II collagen. Scaffolds were characterized prior to seeding with MSCs. The constructs were analyzed for cell binding kinetics, numbers, distribution and viability. Cell attachment and distribution were improved on chitosan coated with type II collagen. MSCs adhered less to reacylated-chitosan and collagen coating did not improve MSCs attachment on those scaffolds. These findings are promising and encourage the evaluation of the differentiation of MSCs in collagen-coated chitosan scaffolds. However, the decreased cell adhesion on reacylated chitosan scaffold seems difficult to overcome and will limit its use for tissue engineering.

## 1 Introduction

Tissue engineering is a rapidly developing field offering new perspectives in the treatment of damaged or diseased tissues. The basic premise of tissue engineering relies on the use of scaffolds to encourage cells to proliferate and organize their extracellular matrix (ECM) in order to form ex vivo a clinically functional tissue, exhibiting histochemical, biochemical and biomechanical properties identical to native, healthy tissue. Three key constituents form the basis of a tissue engineering approach, namely, cells, a scaffold, and signaling molecules [1]. The use of mesenchymal stem cells (MSCs) as a cell source is attractive because they can be harvested with less morbidity from a patient than most differentiated cells, [2–4] have self-renewal abilities, and can differentiate into several cell types [4, 5].

The cell behavior will be affected by the chemical composition and structural characteristics of the three-dimensional (3-D) scaffold, which will ultimately determine the performance of the tissue-engineered construct [1, 6–8]. The biocompatibility of biomaterials derived from chitin and their similarity to the glycosaminoglycans (GAG) naturally present in extracellular matrix make them particularly attractive as a candidate for skeletal tissue engineering [9]. Chitosan is the second most abundant natural polysaccharide, primarily obtained as a subproduct of shellfish by deacetylation of chitin [10]. Chitin and chitosan have been studied for use in a number of biomedical applications including wound dressings, drug delivery systems, and space filling implants and has gained FDA approval for human use [11, 12]. These biomaterials can be molded in various geometries and forms including fibrous scaffolds which have biomimetic properties [13–16]. Considerable attention has recently focused on chitosan and its

---

G. R. Ragetly (✉) · D. J. Griffon  
Department of Veterinary Clinical Medicine,  
University of Illinois, Urbana, IL 61802, USA  
e-mail: ragetly2@illinois.edu

H.-B. Lee  
Department of Veterinary Medicine, Chonbuk National  
University, Jeonju, Republic of Korea

Y. S. Chung  
Department of Textile Engineering, Chonbuk National  
University, Jeonju, Republic of Korea

applications in the field of skeletal tissue engineering including cartilage, intervertebral disk, and bone [11, 13–20]. We have previously reported improved chondrogenesis but limited adhesion of chondrocytes and MSCs on chitosan sponges and meshes [15, 16, 21]. Others have confirmed these results, limiting the application of chitosan and chitin for tissue engineering [22–24]. The initial attachment of cells to a scaffold is a prerequisite for a successful tissue engineering outcome as it is the clincher of cell–matrix interactions [25]. Improving cell attachment and cell distribution on chitosan-derived scaffolds is therefore essential for in vitro cultivation of clinically relevant constructs.

The strategies most commonly employed to improve cell adhesion on biomaterials focus on reduction of non-specific protein adsorption by molecular modification of the biomaterial or immobilization of adhesion molecules to ensure controlled interaction between the cells and the scaffold [26]. The effect of specific molecules on cell adhesion is dependent on the chemical modification, the bulk biomaterial, and the type of cells evaluated [27]. The peptide Arg-Gly-Asp (RGD) is the coating agent most often used to promote the attachment of cells on material surfaces [28, 29]. However, RGD was found to inhibit fibroblast adhesion and proliferation on reacylated chitosan films [26]. Moreover, the immobilization of synthetic RGD affects the ability of MSCs to differentiate [30]. Type II collagen is another candidate which could improve cell attachment via the interactions with the integrins  $\alpha 1$ ,  $\alpha 2$ ,  $\alpha 10$ , and/or  $\alpha 11 \beta 1$  as well as the discoidin-domain receptors, and the annexin V receptor [31–34]. Type II collagen has been less commonly used for tissue engineering applications than type I collagen. Although type I collagen coating has been found to improve cell adhesion on chitosan, the use of type II collagen is more attractive as a biomimetic strategy to improve both MSCs adhesion and chondrogenic or osteogenic differentiation [35, 36]. Type II collagen differs from type I collagen in structure, distribution, and effects on cells [37, 38]. Type I collagen can be found in skeletal tissue but also in skin, cornea, arteries, internal organs, and granulation tissues whereas the natural distribution of type II collagen is more specific to skeletal tissues (hyaline cartilage, bone growth plate). In one study, chondrocyte proliferation and distribution were improved in type II collagen matrices compared to type I collagen matrices [39]. Type II collagen as a bulk biomaterial has been used in few tissue engineering applications [39–43]. Scaffolds composed of bulk type II collagen-poly-caprolactone improved chondrocyte adhesion and proliferation compared to poly-caprolactone scaffolds [41]. Although the mechanical properties and dimensional stability of type II collagen prevent its use as a bulk biomaterial, they do not affect its potential as a coating molecule for scaffolds used in skeletal tissue

engineering [42]. To our knowledge, the evaluation of type II collagen coating has only been limited to one study on poly-lactide-coglycolide scaffolds [42]. The effect of type II collagen coating on chitosan and reacylated chitosan scaffolds has not been evaluated.

The objectives of this study were to determine the extent to which reacylation of chitosan and/or type II collagen coating could improve MSCs seeding. We hypothesized that MSCs adhesion will be greater on chitosan meshes compared to reacylated chitosan meshes and that type II collagen coating will improve cell seeding efficiency on both chitosan and reacylated chitosan scaffolds.

## 2 Materials and methods

### 2.1 Scaffolds

The chitosan (Texanmedtecho, Korea) used in this study has a molecular weight of 480 kDa, a degree of deacetylation of 92% and a viscosity of 370 cP at a 0.5% concentration. Chitosan powder was dissolved and stirred at room temperature for 48 h in 2 wt% aqueous acetic acid solution to obtain a 4 wt% chitosan solution.

Chitosan fibrous scaffolds were prepared using a wet spinning method previously reported. The chitosan solution was pumped into a 0.1 mm  $\times$  1,500 holes spinneret using the geared metering pump. To solidify the chitosan solution, the spinneret was immersed in an aqueous coagulation bath containing 10% sodium hydroxide. After exiting the coagulation bath, fibers were washed in alternative hot and cold water baths. Fibers were cut by 51 mm and carded to obtain the chitosan fibers web. The web was bonded by passing through the water-jet chamber and dried. Chitosan fibrous scaffolds were cut to measure 4 mm in diameter and 1.5 mm in height (group 1).

A portion of the chitosan fibers was reacylated by suspension in 150 ml of methanol and acetic anhydride (1 mol per glucosamine unit). The mixture was stirred at 40°C for 24 h. The treated fibers were washed several times with 100% ethanol, and air-dried. Fibers were cut by 51 mm and carded to obtain the reacylated chitosan fibers web. The web was bonded by passing through the water-jet chamber and dried. Reacylated chitosan fibrous scaffolds were cut to measure 4 mm in diameter and 1.5 mm in height (group 2).

Two types of type II collagen solutions were used to coat the scaffolds. Solution 1 was obtained by dissolving 10 mg of type II collagen (Calf type II collagen, Elastin products company, Owensville, Missouri, USA) in 10 ml of 0.4 mg/ml of acetic acid. The two types of scaffolds (chitosan and reacylated chitosan) were placed in solution 1 for 1 h. The chitosan scaffolds dissolved in the collagen solution.

The reacylated chitosan scaffolds were freeze-dried (group 3). Solution 2 was obtained by adding ethanol to solution 1 at a concentration of 3 mg/ml to prevent dissolution of chitosan scaffolds. The two types of scaffolds (reacylated chitosan (group 4) and chitosan (group 5)) were kept in solution 2 for 1 h and dried at room temperature.

A total of 30 scaffolds were prepared for each of the following groups:

1. chitosan scaffolds
2. collagen-coated chitosan scaffolds
3. reacylated chitosan scaffolds
4. collagen-coated reacylated chitosan scaffolds (without ethanol)
5. collagen-coated reacylated chitosan scaffolds (with ethanol).

All scaffolds had a dry weight of  $1.98 \pm 0.18$  mg. They were sterilized with ethylene oxide gas and rehydrated through a series of ethanol/phosphate buffered saline (PBS) solutions (100, 95, 75, 50, 0% ethanol) [44]. The scaffolds were subsequently incubated at 37°C on a shaker incubator in Dulbecco's modified Eagle's medium (DMEM, ATCC, Manassas, VA, USA) for 2 h prior to cell seeding [16].

## 2.2 Mesenchymal stem cells

A mesenchymal cell line (D1 ORL UVA, ATCC) derived from a multipotent mouse bone marrow stromal precursor was used for this study. Complete culture medium consisted of DMEM containing 4.5 g/l glucose (ATCC), supplemented with 10% fetal bovine serum (ATCC), 100 U/ml penicillin, and 100 µg/ml streptomycin (Sigma, St. Louis, MO). Cells were harvested at their fourth passage and suspended in medium prior to seeding. A cell suspension containing  $1.0 \times 10^6$  cells in 20 µl of medium was dropped on the surface of each scaffold (15 scaffolds per group, 5 groups) and placed in untreated six-well non-tissue culture plates. Each construct was allowed to incubate at 37°C for 1 h. After 1 h, 4 ml of culture medium was added to each well and the plates were placed on a platform shaker oscillating starting at 30 rpm and increased to 60 rpm after 3 h. The constructs were maintained at 37°C and 5% CO<sub>2</sub> in culture medium for 24, 48, or 72 h.

## 2.3 Evaluation of the scaffolds

### 2.3.1 Fourier-transform infrared spectroscopy

Fourier-transform infrared (FTIR) spectra of each scaffold type (n = 3) were analyzed by spectrophotometry (Nicolet Nexus FTIR 670, Thermo Electron, Waltham, MA, USA) of dehydrated specimens ground with KBr powder and

compressed into pellets. Element analysis was used to determine the degree of substitution of the *N*-acyl groups and the presence of collagen.

### 2.3.2 Scanning electron microscopy

Each scaffold (n = 2 per group) was mounted and sputter coated with gold–palladium prior to examination with scanning electron microscopy (SEM, Hitachi S4700, Schaumburg, IL, USA) at 1.0 kV. Criteria evaluated included fiber size, surface characteristics, and the presence of type II collagen.

### 2.3.3 Transmission electron microscopy

The scaffolds (n = 2 per group) were fixed in a Karnovsky's Fixative in phosphate buffered 2% Glutaraldehyde and 2.5% Paraformaldehyde. Microwave fixation was used with this primary fixative and the scaffolds were then washed in Sorenson's Phosphate buffer with no further additives. Microwave fixation was also used with the secondary 2% Osmium Tetroxide fixative, followed by the addition of 3% Potassium Ferricyanide for 5 min. After washing with water, saturated Uranyl Acetate was added for 1 h for en bloc staining. The tissue was dehydrated in a series of increasing concentrations of ethanol. Acetonitrile was used as the transition fluid between ethanol and the epoxy. Infiltration series were done with an epoxy mixture using the epon substitute Lx112. The resulting blocks were polymerized at 90°C overnight and trimmed. Transverse (n = 3) and longitudinal (n = 3) sections of 0.35 µm were cut with diamond knives in each specimen. Light microscopy slides were made with one transverse and one longitudinal section and stained with Toluidine Blue O and Basic Fuchsin. Transmission electron microscopy (TEM) sections (two transverse and two longitudinal sections) were stained with Uranyl Acetate and Lead Citrate, and examined with a Transmission Electron Microscope (Hitachi H600, Schaumburg, IL, USA). Criteria evaluated included homogeneity of the fiber size, presence of a coating at their surface and homogeneity of the coating.

### 2.3.4 Type II collagen content

Type II collagen content per scaffold (n = 3 per group) was determined by an enzyme linked immunosorbent assay (ArthroGen-CIA<sup>®</sup> Native Type II Collagen Detection Kit, Chondrex, Redmond, WA) after digestion of the scaffold in pepsin and elastase [16]. Collagen fibrils were solubilized with pepsin and further digested with pancreatic elastase. The optical density of the reacted collagen with monoclonal antibody was read at 490 nm [16].

### 2.3.5 Water content and porosity

Scaffolds ( $n = 5$  per group) were weighed before and after dehydration to determine their wet and dry weights, respectively. The water content was subsequently calculated as:

$$\text{Water content(\%)} = \left( \text{Weight}_{\text{wet}} - \text{Weight}_{\text{dry}} \right) / \text{Weight}_{\text{wet}}$$

The porosity was calculated using the equation: [41]

$$\text{Porosity(\%)} = \left[ \left( \text{Weight}_{\text{wet}} - \text{Weight}_{\text{dry}} \right) / \text{Water density} \right] / \text{Sample volume}$$

The sample volume was  $0.03 \text{ cm}^3$  for all scaffolds. The water density was considered  $1 \text{ g/cm}^3$ .

### 2.3.6 Mechanical property measurement of the chitosan and reacylated chitosan scaffolds

The tensile properties of the scaffolds were evaluated according to ASTM D-5035 using universal instron tester (Model LR5kPlus, Lloyd instrument Co.). The chitosan and reacylated chitosan scaffolds were cut to  $100 \times 25 \text{ mm}$ . Five specimens were tested for each groups. A 5 N load cell was used at a constant rate of  $100 \text{ mm/min}$ . The same tests were repeated after the scaffolds were placed in PBS buffer solution at  $37^\circ\text{C}$  for 1, 2, and 3 weeks. The breaking strength was measured to evaluate the change of bulk properties and mechanical stability.

## 2.4 Evaluation of constructs

### 2.4.1 Evaluation of cell binding kinetics and cell viability

Cell binding kinetics and viability were evaluated after the initial incubation phase, once fresh media was added to each well. The number of cells suspended in medium and their viability were evaluated at 1, 2, 4, 6, 18 and 22 h after the initial seeding via trypan blue exclusion. Measurements were taken separately for each scaffold type among two wells. The cell concentration in the medium was compared for each time point [45].

### 2.4.2 Live/dead assay

The viability of cells in the constructs 48 h after seeding was determined using the Live/Dead Viability/Cytotoxicity Kit (Molecular Probes, Carlsbad, CA, USA) according to the manufacturer's protocol. Constructs ( $n = 2$  per group) were washed three times in sterile PBS for 2 min, placed on a glass slide, and immersed in  $200 \mu\text{l}$  of PBS solution

containing 2 mM calcein AM and 4 mM ethidium homodimer 1 prior to incubation for 40 min at room temperature. Confocal microscopy (Olympus BX50 Confocal Microscope, Olympus, Center Valley, PA, USA), using Melles Griot Argon and Krypton lasers at excitation wavelengths of 488 and 568 nm, allowed the visualization of calcein AM (labeling live cells = green fluorescence) and ethidium homodimer-1 (labeling dead cells = red fluorescence). The intensities of viable and dead cells were recorded on four field of view at a magnification of  $40\times$ . The slides were analyzed using a specific software (Fluoview, Olympus) to determine the percentage of viable cells.

### 2.4.3 Weights, water, and DNA content

Constructs were weighed 24 ( $n = 5$  per group) and 72 ( $n = 5$  per group) hours after seeding before and after dehydration to determine their wet and dry weights, respectively. The water content was subsequently calculated. After dehydration, the constructs were assayed for their DNA contents. Samples were digested in papain (Sigma Inc., St-Louis, MO, USA) for 16 h at  $60^\circ\text{C}$ . A fluorometric assay with Hoechst 33258 was used to evaluate DNA content [46]. The cell seeding efficiency was calculated as a ratio between the numbers of cells contained in constructs after 24 h of culture compared to the number of cells initially seeded on each scaffold. The number of cells contained in the constructs was calculated using the average DNA content per cell ( $5.34 \text{ pg}$  per cell) as evaluated by fluorometric assay at the time of cell seeding on cell suspensions containing  $1 \times 10^6$  and  $2 \times 10^6$  cells [16].

The number of cells present in the well unattached to a scaffold was evaluated by DNA quantification 24 ( $n = 2$  per group) and 72 ( $n = 2$  per group) hours after seeding. The cell-media solutions were collected and centrifuged at  $250 \text{ rpm/rcf}$  for 10 min and the pellet was assayed for DNA content using the above protocol.

### 2.4.4 Transmission electron microscopy

The evaluation protocol used for the constructs was similar to that described above for the scaffolds. One construct per group was evaluated at 24, 48, and 72 h after seeding. Criteria evaluated via TEM included cell morphology, cell size, cell attachment to the support, and presence of cytoplasmic extensions.

### 2.4.5 Histology

Light microscopy slides were made following the same protocol as described above for TEM evaluation of the scaffolds. Histological sections were stained with

Toluidine Blue O and Basic Fuchshine and evaluated to assess the cell distribution.

The constructs ( $n = 2$  per group at 72 h) were fixed in 10% neutral buffered formalin, embedded in plastic and cut via microtome to produce three 8  $\mu\text{m}$ -thick sections (one superficial, one in the middle, and one at the bottom) [47]. Sections were stained with a trichrome stain. Slides were examined for cell morphology, cell distribution within slides and between slides of the same construct, and integrity of the scaffold.

#### 2.4.6 Scanning electron microscopy

Constructs were fixed in a 2.5% glutaraldehyde solution in a sodium cacodylate buffer for 2 h. After rinsing with the sodium cacodylate buffer, they were submerged in 1% osmium tetroxide in 0.1 M sodium cacodylate for 90 min. Following a buffer rinse, the constructs were dehydrated through an ethanol series. Finally, constructs were placed in hexamethyldisilazane for 45 min and left under a fume hood until completely dry. A total of two sections per construct (surface and bottom,  $n = 2$  per group at 72 h) were mounted for each construct and sputter coated with gold–palladium prior to examination with SEM at 1.0 kV. Criteria evaluated included cell attachment to the support, presence of cytoplasmic extensions, cell density, and integrity of the scaffold.

#### 2.5 Statistical analysis

Dry and wet weights, increase in dry weight, water contents, cell counts in medium, cell viability, DNA content, and increase in DNA content between 24 and 72 h were compared between the five groups with a risk factor of less than 0.05 considered statistically significant. All data were expressed as mean  $\pm$  standard deviation. Statistical differences were evaluated between the groups with an

ANOVA using Systat 11.0 statistical software (Wilkinson). A t-test was performed to compare the mechanical properties of the chitosan and reacylated chitosan scaffolds. Post-hoc analyses were performed with the LSD test.

### 3 Results

#### 3.1 Evaluation of the scaffolds

##### 3.1.1 FTIR

The degree of acetylation (DA) was 8% for the chitosan scaffolds and 96% for the reacylated chitosan scaffolds. The presence of collagen was confirmed by the presence of bands typical of amide I ( $1658\text{ cm}^{-1}$ ), amide II ( $1552\text{ cm}^{-1}$ ), and amide III ( $1240\text{ cm}^{-1}$ ) (Fig. 1) [48].

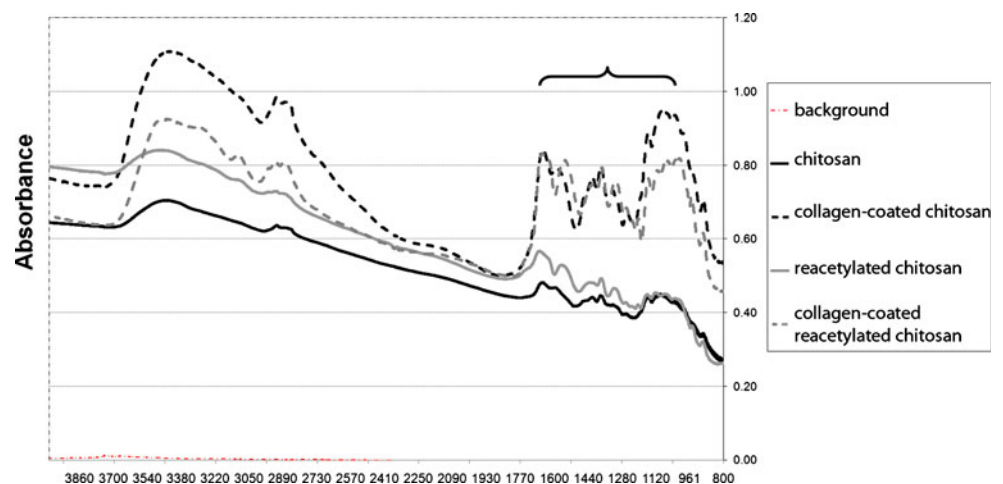
##### 3.1.2 Scanning electron microscopy

All fibers had a diameter of 13–15  $\mu\text{m}$ . They appeared homogeneous within scaffolds and among the different groups. The difference between chitosan and collagen was difficult to distinguish because of similar contrast with SEM evaluation.

##### 3.1.3 Transmission electron microscopy

All fibers appeared of similar size among all TEM samples. A layer of collagen was observed at the surface of the fibers in all collagen-coated scaffolds (Fig. 2). No difference in coating was observed between the center and the periphery or between scaffolds. Aggregation of collagen molecules was observed occasionally in the center as well as in the periphery and in all types of collagen-coated scaffolds (Fig. 2).

**Fig. 1** Fourier transform infrared spectroscopy results. The element analysis was used to determine the degree of substitution of the *N*-acyl groups. The presence of collagen was confirmed in the coated scaffolds by the presence of bands typical of amide I, II, and III (brace)



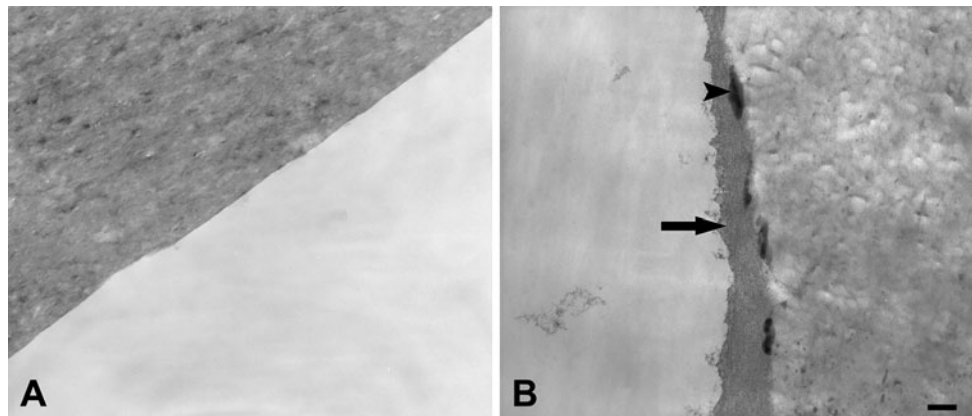


**Fig. 2** Transmission electron microscopy of the edge of a fiber from a chitosan scaffold (**A**) and a collagen-coated chitosan scaffold (**B**). The black arrow indicates the collagen layer seen at the surface of the

collagen-coated chitosan fiber; the arrowhead indicates an aggregation of collagen molecules (magnification x50000). Scale bar: 0.1  $\mu$ m

### 3.1.4 Type II collagen content

Type II collagen was not detected in the non-coated scaffolds. The type II collagen content was  $4.11 \pm 1.39$   $\mu$ g/mg for the collagen-coated chitosan scaffolds,  $4.98 \pm 0.15$   $\mu$ g/mg for the collagen-coated reacylated chitosan scaffolds (without ethanol), and  $8.04 \pm 2.00$   $\mu$ g/mg for the collagen-coated reacylated chitosan scaffolds (with ethanol). The collagen-coated reacylated chitosan scaffolds contained more type II collagen than the collagen-coated chitosan and the collagen-coated reacylated chitosan (without ethanol) scaffolds ( $P = 0.032$  and  $0.044$ , respectively).

### 3.1.5 Water content and porosity

No difference was found in water content nor porosity among groups (mean values among the different groups of  $92.5 \pm 1.8\%$ ,  $P = 0.653$  and  $86.4 \pm 20.7\%$ ,  $P = 0.524$ , respectively) (Table 1).

### 3.1.6 Mechanical property measurement of the chitosan and reacylated chitosan scaffolds

No difference in stress, strain and maximum load to failure was found between the chitosan and reacylated chitosan scaffolds (Table 2).

**Table 1** Summary statistics of the scaffold water content and porosity, the construct water content, and the cell seeding efficiency of the scaffolds or constructs

Composition	Chitosan	Collagen-coated chitosan (ethanol)	Reacylated chitosan	Collagen-coated reacylated chitosan	Collagen-coated reacylated chitosan (ethanol)
Scaffold water content (%)	$92.9 \pm 1.7$ A	$92.7 \pm 1.8$ A	$92.7 \pm 1.4$ A	$92.5 \pm 1.1$ A	$92.5 \pm 1.8$ A
Scaffold porosity (%)	$87.2 \pm 19.0$ A	$91.8 \pm 22.6$ A	$93.7 \pm 20.0$ A	$84.1 \pm 19.8$ A	$85.1 \pm 20.6$ A
Construct water content (%)	$90.0 \pm 2.0$ A	$91.9 \pm 3.0$ A	$91.4 \pm 2.4$ A	$90.3 \pm 1.2$ A	$90.4 \pm 3.9$ A
Cell seeding efficiency (%)	$47.2 \pm 8.6$ B	$81.8 \pm 32.5$ A	$25.5 \pm 10.7$ C	$24.6 \pm 3.6$ C	$23.5 \pm 6.4$ C

A, B, C: groups with different letters differ statistically ( $P < 0.05$ )

**Table 2** Mechanical properties and stability of the chitosan and reacylated chitosan scaffolds

		Week 0	Week 1	Week 2	Week 3
Chitosan scaffold	Maximum load (N)	5.27	5.24	5.13	5.24
	Stress (N/mm)	0.410	0.407	0.394	0.402
	Strain (%)	48.6	50.5	38.2	51.6
Reacylated chitosan scaffold	Maximum load (N)	5.30	5.21	5.12	5.06
	Stress (N/mm)	0.415	0.409	0.398	0.395
	Strain (%)	34.8	35.6	35.8	21.6

## 3.2 Evaluation of constructs

### 3.2.1 Evaluation of cell binding kinetics and cell viability

Cell death in the medium was negligible (less than 5%) throughout the experiment for all seeding techniques as assessed by trypan blue exclusion. Less than 10% of the cells remained in suspension 1 h after the seeding for all scaffold types. No difference in cell concentration was found until 6 h after seeding. More cells remained in suspension in the wells of the chitosan scaffolds than in other groups 6 h after seeding ( $P = 0.014$ ) but this difference was not found at any later time points ( $P > 0.497$ ).

### 3.2.2 Live/dead assay

The viability of the MSCs estimated by a live/dead fluorescent assay 48 h after seeding did not differ among the five groups and remained above 83.6% for all constructs ( $93.9\% \pm 8.9$ ,  $P = 0.447$ ).

### 3.2.3 Weights, water, and DNA content

No difference was found between groups in wet weight, dry weight and water content after seeding ( $P = 0.249$ ,  $0.403$ , and  $0.432$ , respectively). The water content was  $90.8 \pm 2.6\%$  (Table 1).

The DNA remained stable within groups from 24 to 72 h after seeding ( $P > 0.172$  for all scaffold types). The average DNA content was  $2.51 \pm 0.46 \mu\text{g}$  for the chitosan constructs,  $4.37 \pm 1.73 \mu\text{g}$  for the collagen-coated chitosan constructs,  $1.36 \pm 0.57 \mu\text{g}$  for the reacylated chitosan constructs,  $1.32 \pm 0.19 \mu\text{g}$  for the collagen-coated reacylated chitosan constructs (without ethanol), and  $1.25 \pm 0.34 \mu\text{g}$  for the collagen-coated reacylated chitosan constructs (with ethanol) (Fig. 3). The collagen-coated chitosan constructs contained more DNA than any other constructs at 24 and 72 h ( $P < 0.001$  for all comparisons). Chitosan constructs contained more DNA than the collagen-coated

reacylated chitosan constructs at 24 h ( $P = 0.030$  and  $0.045$ ) and than all reacylated chitosan constructs at 72 h ( $P = 0.002$ – $0.004$ ). No difference was found between the reacylated chitosan constructs at either 24 or 72 h ( $P > 0.696$  and  $P > 0.856$ , respectively). The cell seeding efficiency after 24 h of culture was  $47.2 \pm 8.6\%$  for the chitosan constructs,  $81.8 \pm 32.5\%$  for the collagen-coated chitosan constructs,  $25.5 \pm 10.7\%$  for the reacylated chitosan constructs,  $24.6 \pm 3.6\%$  for the collagen-coated reacylated chitosan constructs (without ethanol), and  $23.5 \pm 6.4\%$  for the collagen-coated reacylated chitosan constructs (with ethanol) (Table 1). The efficiency of cell seeding was greater on collagen-coated chitosan scaffolds than any other construct ( $P < 0.001$  for all comparisons). Seeding was improved on chitosan scaffolds compared to all reacylated chitosan constructs ( $P = 0.016$ – $0.034$ ). No difference was detected among the different reacylated chitosan constructs ( $P > 0.9$ ).

No difference in the DNA content of the well was found after 24 h ( $P = 0.588$ ). However, the DNA content of the wells of chitosan constructs was greater than the one of the wells of all other constructs at 72 h ( $P = 0.014$ ).

### 3.2.4 Transmission electron microscopy

Cells exhibited similar morphological features typical of mesenchymal stem cells including a spindle-shape and elliptical nucleus with usually multiple nucleoli, various mitochondrial profiles, and small vacuoles. No difference in cell morphology was observed between the constructs at 24, 48, and 72 h after seeding. No difference in cell attachment could be observed between the different groups.

### 3.2.5 Histology

The cell density and distribution among each construct was assessed with the histological sections stained with Toluidine Blue O and Basic Fuchsin. Findings were in agreement with those of DNA content. The cell distribution also appeared to differ among groups (Fig. 4). Cells in chitosan constructs tended to be grouped rather than uniformly distributed, whereas cell distribution seemed more uniform in collagen-coated chitosan constructs. Although less obvious, a similar trend was observed in reacylated chitosan constructs where cells appeared more uniformly distributed along collagen-coated fibers. Examination of the samples stained with trichrome confirmed the findings obtained with the light microscopy slides of the TEM in terms of subjective cell numbers and distribution among groups. Cells exhibited the appearance of MSCs in all constructs (Fig. 5). The chitosan structure appeared intact in all constructs.

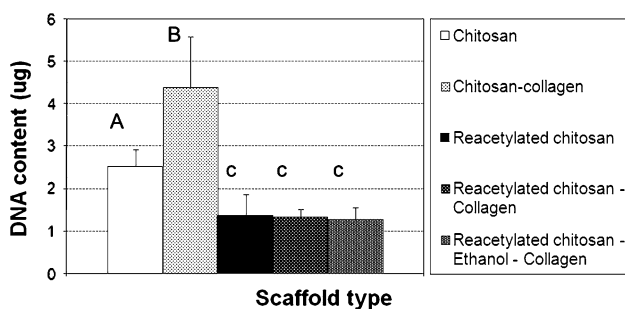


**Fig. 3** Average DNA content of the constructs 24 and 72 h after seeding. A, B, C groups with different letters differ statistically ( $P < 0.05$ )

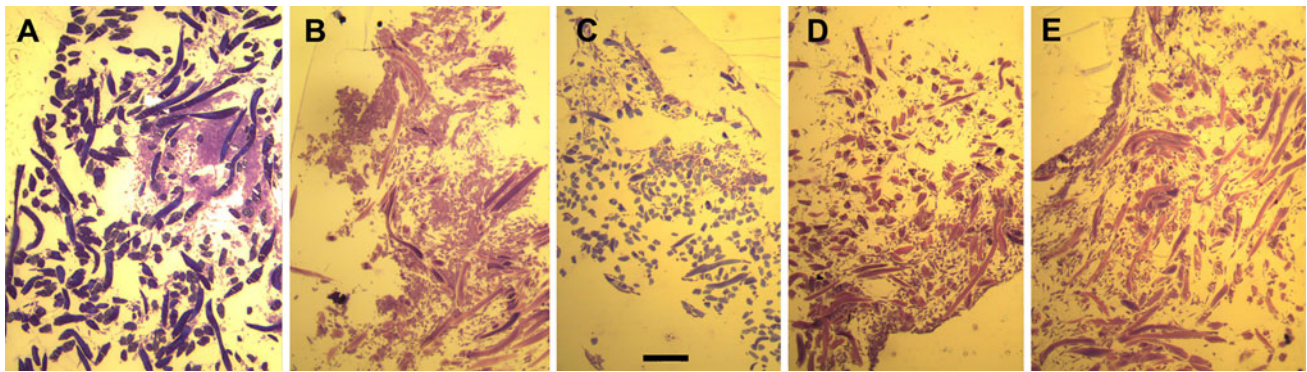
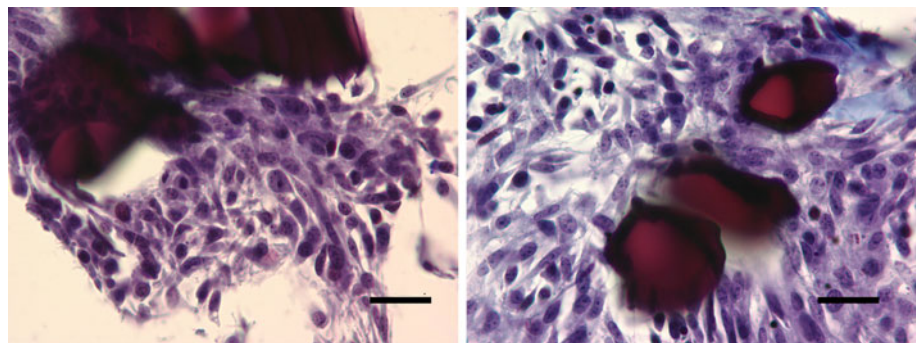


**Fig. 4** Histological analysis with toluidine blue O and basic fuchsin 24 h after seeding allowing evaluation of cell distribution within each construct. **A** Chitosan constructs. **B** Collagen-coated chitosan constructs. **C** Reacylated chitosan constructs. **D** Collagen-coated

reacylated chitosan constructs (without ethanol). **E** Collagen-coated reacylated chitosan constructs (with ethanol) (magnification  $\times 10$ , bar 100  $\mu\text{m}$ )

**Fig. 5** Histological analysis with trichrome stain 72 h after seeding of a chitosan construct (*left*) and a collagen-coated chitosan construct (*right*). Cells exhibited the appearance of MSCs and were well attached to the scaffold (magnification  $\times 100$ , bar 30  $\mu\text{m}$ )



### 3.2.6 Scanning electron microscopy

Most MSCs exhibited a spindle-shape with prominent cytoplasmic extensions. No major differences in cell morphology were observed among groups. The cells tended to be uniformly distributed within each evaluated surface (surface or bottom). However, marked differences in cell density were observed and were in agreement with those of DNA content (Fig. 6). The reacylated chitosan constructs contained fewer cells at the surface and at the bottom than the chitosan-based constructs. More cells were present at the surface and at the bottom of collagen coated chitosan constructs than in all the other groups. It was not possible to count the cells because they exhibited a spindle-shape with prominent cytoplasmic extensions and tended to form sheets [15, 16]. Finally, the structural integrity of fibers seemed intact in all groups.

## 4 Discussion

The initial attachment of cells during seeding is a prerequisite for a successful tissue engineering outcome as it is

the clincher of cell–matrix and cell–cell interactions [25]. Modifying chitosan scaffolds to optimize cell adhesion within the 3-D matrices is crucial to improve seeding yield and uniformity of cell distribution. The main findings of this study are that: (1) chitosan fibrous scaffolds can be chemically modified to alter their DA and/or their type II collagen coating, (2) type II collagen coating on chitosan fibrous scaffolds improves cell adhesion and cell distribution during seeding, and (3) increasing the degree of acetylation of chitosan scaffolds limits cell adhesion which cannot be effectively overcome by type II collagen coating.

Considerable attention has recently focused on chitosan scaffolds but their use has been limited because of their deficient properties for cell adhesion [22–24]. Our results confirm the low seeding efficiency of chitosan scaffolds (47.2%) seeded with MSCs. Histology, SEM and TEM evaluations correlated with the quantitative analysis. Cells seem to display greater affinity for each other than for the surface of chitosan fibers, forming clusters that contributed to the uneven cell distribution within constructs. The structure, wettability and porosity of scaffolds were consistent with previous reports [49]. The variability in porosity between the scaffolds may reflect scaffold variation



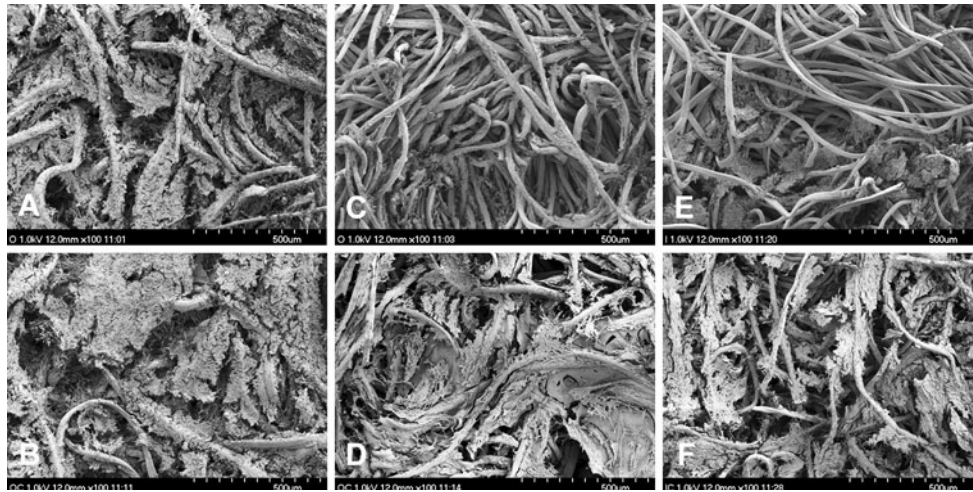


**Fig. 6** Scanning electron microscopy of the constructs 72 h after seeding with MSCs. **A** Surface of a chitosan construct. **B** Surface of a collagen-coated chitosan construct. **C** Bottom of a chitosan construct.

**D** Bottom of a collagen-coated chitosan construct. **E** Surface of a reacylated chitosan construct. **F** Surface of a collagen-coated reacylated chitosan construct (magnification  $\times 100$ )

or lack of precision of the measurement technique. The variation is more likely due to the technique since the scaffolds had the same structure on SEM evaluation and a low variability in their dry weight. This technique was used because the equation was found to be reliable to assess the porosity [41]. Coating chitosan fibers with type II collagen did not affect the structural properties of the scaffolds but improved cell adhesion. This structural similarity between scaffolds allows direct evaluation of the effect of chemical composition (collagen coating) on cell seeding [50, 51]. The coating did not impact cell viability but increased the cell seeding efficiency by 73%. The greater numbers of cells unattached to chitosan scaffolds in the medium (at 6 h) and in the well (at 72 h) compared to the collagen-coated chitosan scaffolds supports the effect of type II collagen on cell attachment. Type II collagen coating also improved cell distribution in collagen-coated constructs improving attachment to fibers rather than formation of clusters compared to chitosan constructs. These effects may be attributed to the presence binding sites in type II collagen, such as the amino acid sequences GFOGER and RGD. These binding sites have been found to promote cell attachment by the integrins  $\alpha 1$ ,  $\alpha 2$ ,  $\alpha 10$ , and/or  $\alpha 11\beta 1$ , the discoidin-domain receptors, and the annexin V receptor [31–34]. The adhesion of the cells to the matrix is believed to act as a clincher for intracellular signals, influencing subsequent cell–matrix interaction and cell differentiation [25, 32]. Type II collagen could therefore also improve the differentiation of the MSCs to form skeletal tissue. In fact, the synergistic effect of growth factors and extracellular type II collagen on Smad 2 phosphorylation has been shown to increase the level of ECM mRNA expression [52, 53]. Also, chondrogenic differentiation and endochondral ossification proceed through

condensation. This formation of cell clusters due to increased cell density secondary to type II collagen coating can promote cadherin-mediated cell–cell interactions for skeletal tissue engineering. Future studies should be conducted to evaluate the chondrogenic and/or osteogenic differentiation of MSCs in the type II collagen coated chitosan scaffolds.

The influence of deacetylation of chitosan on cell attachment remains controversial and varies between reports and cell types [54]. In several studies, deacetylation improved the attachment of fibroblasts, Schwann cells, keratinocytes, and neurons to chitosan films or sponges [22–24, 55–57]. However, in others, a greater degree of acetylation of chitosan did not affect the attachment of chondrocytes, fibroblasts, or osteoblasts [58–61]. These conflicting results may be due to differences in origin, molecular weight, and/or viscosity of the agents tested (chitosan, chitin, re-acetylated chitosan) as well as differences in experimental design such as cell population and serum supplementation [60, 61]. We describe for the first time a decreased cell attachment of MSCs on reacylated chitosan scaffolds (DA: 96%) compared to chitosan (DA: 8%). The scaffolds were produced from the same source of chitosan to avoid variation due to characteristics other than DA. Cells were seeded in medium containing serum, routinely recommended for culture of MSCs. The inverse relationship between adhesion of MSCs and the DA of chitosan scaffolds could be explained by several possible mechanisms. It was first suspected that the amine groups of the deacetylated form of chitosan would remain protonated to  $-\text{NH}_3^+$  in media, resulting in a cationic nature primarily responsible for electrostatic interactions between protonated amine groups and negatively charged cell surfaces [55,

61]. However, the majority of the ammonium groups become dissociated and subsequently uncharged when the medium reaches a pH close to the pK<sub>A</sub> of chitosan (6.46–6.8) [22]. This explains why the zeta potentials of chitosan films were null or slightly positive in neutral medium and not affected by the DA [62]. The cell adhesion characteristics of the chitosan may therefore not be directly related to direct cell–matrix interactions but instead, correlate with the differential adsorption of proteins present in the culture medium to the biomaterial [63]. Although no correlation has yet been established between the adsorption of type II collagen and the DA of scaffolds, the mechanism of protein adsorption in media containing serum most likely differs from that of single protein adsorption in acidic conditions. Chitosan with a low DA may accelerate cell adhesion after forming polyelectrolyte complexes with serum components such as heparin, platelet-derived growth factor, laminin, or fibronectin [64, 65]. Chitosan with a lower DA can bind more growth factors in the serum and protect them from degradation and/or present them to the cells in an active form [65, 66]. This could potentially explain the absence of effect of the DA on fibroblast attachment and proliferation found by Hamilton et al. in serum free media [60]. The DA of chitosan scaffolds has been shown to impact the final constructs in skeletal tissue engineering applications. Several studies have reported improved characteristics of the extracellular matrix produced by chondrocytes, [58, 59] or osteoblasts [22, 61] when these cells were cultured on chitosan scaffolds of higher DA. These publications justify our attempts to overcome the poor cell adhesion on chitin and reacylated chitosan [55, 56, 60]. Type II collagen did not improve the overall cell seeding efficiency of reacylated chitosan constructs. Even if the cell distribution appeared more homogeneous in the collagen-coated constructs, the poor adhesion properties of reacylated chitosan seem difficult to overcome.

## 5 Conclusions

Reacylation of chitosan fibers was detrimental to the attachment and the distribution of MSCs, regardless of collagen coating. Cell adhesion on reacylated chitosan scaffolds seems difficult to overcome and will likely limit its clinical application. Type II collagen coating improved MSCs adhesion and distribution on chitosan fibers but had no effect on reacylated chitosan scaffolds. The seeding efficiency of 82% and the high kinetic rate of the collagen-coated chitosan scaffolds meet the criteria for application in tissue engineering. These findings are promising and encourage the evaluation of the differentiation of MSCs in chitosan fibrous scaffolds coated with type II collagen. However, future studies should evaluate the differentiation

of MSCs in chitosan fibrous scaffolds coated with type II collagen to assess its biomimetic properties for cartilage and/or bone tissue engineering applications.

**Acknowledgment** Project no. s-08-83G was supported by the AO Research Fund of the AO Foundation and the ACVS Foundation.

## References

- Athanasίου KA, Shah AR, Hernandez RJ, LeBaron RG. Basic science of articular cartilage repair. *Clin Sports Med.* 2001;20:223–47.
- Fortier LA. Stem cells: classifications, controversies, and clinical applications. *Vet Surg.* 2005;34:415–23.
- Helder MN, Knippenberg M, Klein-Nulend J, Wuisman PI. Stem cells from adipose tissue allow challenging new concepts for regenerative medicine. *Tissue Eng.* 2007;13:1799–808.
- Gao J, Yao JQ, Caplan AI. Stem cells for tissue engineering of articular cartilage. *Proc Inst Mech Eng.* 2007;221:441–50.
- Caplan AI. Review: mesenchymal stem cells: cell-based reconstructive therapy in orthopedics. *Tissue Eng.* 2005;11:1198–211.
- Li WJ, Jiang YJ, Tuan RS. Chondrocyte phenotype in engineered fibrous matrix is regulated by fiber size. *Tissue Eng.* 2006;12:1775–85.
- Moroni L, Licht R, de Boer J, de Wijn JR, van Blitterswijk CA. Fiber diameter and texture of electrospun PEOT/PBT scaffolds influence human mesenchymal stem cell proliferation and morphology, and the release of incorporated compounds. *Biomaterials.* 2006;27:4911–22.
- Pei M, Solchaga LA, Seidel J, Zeng L, Vunjak-Novakovic G, Caplan AI, Freed LE. Bioreactors mediate the effectiveness of tissue engineering scaffolds. *FASEB J.* 2002;16:1691–4.
- VandeVord PJ, Matthew HW, DeSilva SP, Mayton L, Wu B, Wooley PH. Evaluation of the biocompatibility of a chitosan scaffold in mice. *J Biomed Mater Res.* 2002;59:585–90.
- Chenite A, Chaput C, Wang D, Combes C, Buschmann MD, Hoemann CD, Leroux JC, Atkinson BL, Binette F, Selmani A. Novel injectable neutral solutions of chitosan form biodegradable gels in situ. *Biomaterials.* 2000;21:2155–61.
- Madihally SV, Matthew HW. Porous chitosan scaffolds for tissue engineering. *Biomaterials.* 1999;20:1133–42.
- Khor E, Lim LY. Implantable applications of chitin and chitosan. *Biomaterials.* 2003;24:2339–49.
- Di Martino A, Sittinger M, Risbud MV. Chitosan: a versatile biopolymer for orthopaedic tissue-engineering. *Biomaterials.* 2005;26:5983–90.
- Yamane S, Iwasaki N, Majima T, Funakoshi T, Masuko T, Harada K, Minami A, Monde K, Nishimura S. Feasibility of chitosan-based hyaluronic acid hybrid biomaterial for a novel scaffold in cartilage tissue engineering. *Biomaterials.* 2005;26:611–9.
- Griffon DJ, Sedighi MR, Sendemir-Urkmez A, Stewart AA, Jamison R. Evaluation of vacuum and dynamic cell seeding of polyglycolic acid and chitosan scaffolds for cartilage engineering. *Am J Vet Res.* 2005;66:599–605.
- Griffon DJ, Sedighi MR, Schaeffer DV, Eurell JA, Johnson AL. Chitosan scaffolds: interconnective pore size and cartilage engineering. *Acta Biomater.* 2006;2:313–20.
- Yamane S, Iwasaki N, Kasahara Y, Harada K, Majima T, Monde K, Nishimura SI, Minami A. Effect of pore size on in vitro cartilage formation using chitosan-based hyaluronic acid hybrid polymer fibers. *J Biomed Mater Res A.* 2006;81:586–93.

18. Kasahara Y, Iwasaki N, Yamane S, Igarashi T, Majima T, Nonaka S, Harada K, Nishimura SI, Minami A. Development of mature cartilage constructs using novel three-dimensional porous scaffolds for enhanced repair of osteochondral defects. *J Biomed Mater Res A*. 2008;86:127–36.
19. Jeon YH, Choi JH, Sung JK, Kim TK, Cho BC, Chung HY. Different effects of PLGA and chitosan scaffolds on human cartilage tissue engineering. *J Craniofac Surg*. 2007;18:1249–58.
20. Chen YL, Lee HP, Chan HY, Sung LY, Chen HC, Hu YC. Composite chondroitin-6-sulfate/dermatan sulfate/chitosan scaffolds for cartilage tissue engineering. *Biomaterials*. 2007;28:2294–305.
21. Ragetty GR, Slavik GJ, Cunningham BT, Schaeffer DJ, Griffon DJ. Cartilage tissue engineering on fibrous chitosan scaffolds produced by a replica molding technique. *J Biomed Mater Res A*. 2010;93:46–55.
22. Amaral IF, Cordeiro AL, Sampaio P, Barbosa MA. Attachment, spreading and short-term proliferation of human osteoblastic cells cultured on chitosan films with different degrees of acetylation. *J Biomater Sci Polym Ed*. 2007;18:469–85.
23. Seda Tigli R, Karakecili A, Gumusderelioglu M. In vitro characterization of chitosan scaffolds: influence of composition and deacetylation degree. *J Mater Sci Mater Med*. 2007;18:1665–74.
24. Wenling C, Duohui J, Jiamou L, Yandao G, Nanming Z, Xiufang Z. Effects of the degree of deacetylation on the physicochemical properties and Schwann cell affinity of chitosan films. *J Biomater Appl*. 2005;20:157–77.
25. Mahmood TA, de Jong R, Riesle J, Langer R, van Blitterswijk CA. Adhesion-mediated signal transduction in human articular chondrocytes: the influence of biomaterial chemistry and tenascin-C. *Exp Cell Res*. 2004;301:179–88.
26. Carvalho V, Domingues L, Gama M. The inhibitory effect of an RGD-human chitin-binding domain fusion protein on the adhesion of fibroblasts to reacylated chitosan films. *Mol Biotechnol*. 2008;40:269–79.
27. Wang YC, Kao SH, Hsieh HJ. A chemical surface modification of chitosan by glycoconjugates to enhance the cell-biomaterial interaction. *Biomacromolecules*. 2003;4:224–31.
28. Hersel U, Dahmen C, Kessler H. RGD modified polymers: biomaterials for stimulated cell adhesion and beyond. *Biomaterials*. 2003;24:4385–415.
29. Hubbell JA. *Biomaterials in tissue engineering*. Biotechnology (NY). 1995;13:565–76.
30. Connelly JT, Garcia AJ, Levenston ME. Inhibition of in vitro chondrogenesis in RGD-modified three-dimensional alginate gels. *Biomaterials*. 2007;28:1071–83.
31. Durr J, Goodman S, Potocnik A, von der Mark H, von der Mark K. Localization of beta 1-integrins in human cartilage and their role in chondrocyte adhesion to collagen and fibronectin. *Exp Cell Res*. 1993;207:235–44.
32. Reid DL, Aydelotte MB, Mollenhauer J. Cell attachment, collagen binding, and receptor analysis on bovine articular chondrocytes. *J Orthop Res*. 2000;18:364–73.
33. Gigout A, Jolicœur M, Nelea M, Raynal N, Fardale R, Buschmann MD. Chondrocyte aggregation in suspension culture is FFOGER-GPP- and beta1 integrin-dependent. *J Biol Chem*. 2008;283:31522–30.
34. Freyria AM, Ronziere MC, Cortial D, Galois L, Hartmann D, Herbage D, Mallein-Gerin F. Comparative phenotypic analysis of articular chondrocytes cultured within type I or type II collagen scaffolds. *Tissue Eng Part A*. 2009;15:1233–45.
35. Stevens MM, George JH. Exploring and engineering the cell surface interface. *Science*. 2005;310:1135–8.
36. Lutolf MP, Hubbell JA. Synthetic biomaterials as instructive extracellular microenvironments for morphogenesis in tissue engineering. *Nat Biotechnol*. 2005;23:47–55.
37. Duan Y, Wang Z, Yan W, Wang S, Zhang S, Jia J. Preparation of collagen-coated electrospun nanofibers by remote plasma treatment and their biological properties. *J Biomater Sci Polym Ed*. 2007;18:1153–64.
38. Kim HJ, Lee JH, Im GI. Chondrogenesis using mesenchymal stem cells and PCL scaffolds. *J Biomed Mater Res A*. 2010;92:659–66.
39. Pieper JS, van der Kraan PM, Hafmans T, Kamp J, Buma P, van Susante JL, van den Berg WB, Veerkamp JH, van Kuppevelt TH. Crosslinked type II collagen matrices: preparation, characterization, and potential for cartilage engineering. *Biomaterials*. 2002;23:3183–92.
40. Tsai CL, Hsu SH, Cheng WL. Effect of different solvents and crosslinkers on cytocompatibility of Type II collagen scaffolds for chondrocyte seeding. *Artif Organs*. 2002;26:18–26.
41. Chang KY, Hung LH, Chu IM, Ko CS, Lee YD. The application of type II collagen and chondroitin sulfate grafted PCL porous scaffold in cartilage tissue engineering. *J Biomed Mater Res A*. 2010;92:712–23.
42. Hsu SH, Chang SH, Yen HJ, Whu SW, Tsai CL, Chen DC. Evaluation of biodegradable polyesters modified by type II collagen and Arg-Gly-Asp as tissue engineering scaffolding materials for cartilage regeneration. *Artif Organs*. 2006;30:42–55.
43. Yen HJ, Tseng CS, Hsu SH, Tsai CL. Evaluation of chondrocyte growth in the highly porous scaffolds made by fused deposition manufacturing (FDM) filled with type II collagen. *Biomed Microdevices*. 2009;11:615–24.
44. Marreco PR, da Luz Moreira P, Genari SC, Moraes AM. Effects of different sterilization methods on the morphology, mechanical properties, and cytotoxicity of chitosan membranes used as wound dressings. *J Biomed Mater Res B Appl Biomater*. 2004;71:268–77.
45. Vunjak-Novakovic G, Obradovic B, Martin I, Bursac PM, Langer R, Freed LE. Dynamic cell seeding of polymer scaffolds for cartilage tissue engineering. *Biotechnol Prog*. 1998;14:193–202.
46. Kim YJ, Sah RL, Doong JY, Grodzinsky AJ. Fluorometric assay of DNA in cartilage explants using Hoechst 33258. *Anal Biochem*. 1988;174:168–76.
47. Seddighi MR, Griffon DJ, Schaeffer DJ, Fadl-Alla BA, Eurell JA. The effect of chondrocyte cryopreservation on cartilage engineering. *Vet J*. 2008;178:244–50.
48. Cao H, Xu SY. Purification and characterization of type II collagen from chick sternal cartilage. *Food chemistry*. 2008;108:439–45.
49. Nettles DL, Elder SH, Gilbert JA. Potential use of chitosan as a cell scaffold material for cartilage tissue engineering. *Tissue Eng*. 2002;8:1009–16.
50. Karande TS, Ong JL, Agrawal CM. Diffusion in musculoskeletal tissue engineering scaffolds: design issues related to porosity, permeability, architecture, and nutrient mixing. *Ann Biomed Eng*. 2004;32:1728–43.
51. Malda J, Woodfield TB, van der Vloodt F, Wilson C, Martens DE, Tramper J, van Blitterswijk CA, Riesle J. The effect of PEGT/PBT scaffold architecture on the composition of tissue engineered cartilage. *Biomaterials*. 2005;26:63–72.
52. Schneiderbauer MM, Dutton CM, Scully SP. Signaling “cross talk” between TGF-beta1 and ECM signals in chondrocytic cells. *Cell Signal*. 2004;16:1133–40.
53. Qi WN, Scully SP. Effect of type II collagen in chondrocyte response to TGF-beta 1 regulation. *Exp Cell Res*. 1998;241:142–50.
54. Fakhry A, Schneider GB, Zaharias R, Senel S. Chitosan supports the initial attachment and spreading of osteoblasts preferentially over fibroblasts. *Biomaterials*. 2004;25:2075–9.
55. Chatelet C, Damour O, Domard A. Influence of the degree of acetylation on some biological properties of chitosan films. *Biomaterials*. 2001;22:261–8.

56. Freier T, Koh HS, Kazazian K, Shoichet MS. Controlling cell adhesion and degradation of chitosan films by N-acetylation. *Biomaterials*. 2005;26:5872–8.
57. Tigli RS, Gumusderelioglu M. Evaluation of RGD- or EGF-immobilized chitosan scaffolds for chondrogenic activity. *Int J Biol Macromol*. 2008;43:121–8.
58. Kuo YC, Lin CY. Effect of genipin-crosslinked chitin-chitosan scaffolds with hydroxyapatite modifications on the cultivation of bovine knee chondrocytes. *Biotechnol Bioeng*. 2006;95:132–44.
59. Suzuki D, Takahashi M, Abe M, Sarukawa J, Tamura H, Tokura S, Kurahashi Y, Nagano A. Comparison of various mixtures of beta-chitin and chitosan as a scaffold for three-dimensional culture of rabbit chondrocytes. *J Mater Sci Mater Med*. 2008;19:1307–15.
60. Hamilton V, Yuan Y, Rigney DA, Puckett AD, Ong JL, Yang Y, Elder SH, Bumgardner JD. Characterization of chitosan films and effects on fibroblast cell attachment and proliferation. *J Mater Sci Mater Med*. 2006;17:1373–81.
61. Suphasiriroj W, Yotnuengnit P, Surarit R, Pichyangkura R. The fundamental parameters of chitosan in polymer scaffolds affecting osteoblasts (MC3T3-E1). *J Mater Sci Mater Med*. 2009;20:309–20.
62. Tomihata K, Ikada Y. In vitro and in vivo degradation of films of chitin and its deacetylated derivatives. *Biomaterials*. 1997;18:567–75.
63. Chastain SR, Kundu AK, Dhar S, Calvert JW, Putnam AJ. Adhesion of mesenchymal stem cells to polymer scaffolds occurs via distinct ECM ligands and controls their osteogenic differentiation. *J Biomed Mater Res A*. 2006;78:73–85.
64. Inui H, Tsujikubo M, Hirano S. Low molecular weight chitosan stimulation of mitogenic response to platelet-derived growth factor in vascular smooth muscle cells. *Biosci Biotechnol Biochem*. 1995;59:2111–4.
65. Mori T, Okumura M, Matsuura M, Ueno K, Tokura S, Okamoto Y, Minami S, Fujinaga T. Effects of chitin and its derivatives on the proliferation and cytokine production of fibroblasts in vitro. *Biomaterials*. 1997;18:947–51.
66. Howling GI, Dettmar PW, Goddard PA, Hampson FC, Dornish M, Wood EJ. The effect of chitin and chitosan on the proliferation of human skin fibroblasts and keratinocytes in vitro. *Biomaterials*. 2001;22:2959–66.